

# Novel Plasma Diagnostic Measurement of Electron Temperature and Electron Density Using Tone Burst Wave

Takeshi Katahira, Hiromu Kawana, Mikio Ohuchi, and Shuichi Sato<sup>ID</sup>

**Abstract**—We used the tone burst floating probe method to measure plasma parameters in a hollow cathode discharge. In this method, the electron temperature is directly calculated from a shift in the floating potential of the burst interval when a tone burst signal is applied to a probe through an intermediary blocking capacitor. The tone burst signal is a signal that applies an ac signal for a fixed time and turns off the remaining time of the cycle. It was possible to measure the same electron temperature as in the floating probe method that we previously reported. In the tone burst floating probe method, it is possible to measure the ion current by a shift in the floating potential from the time constant of the burst interval. This is a new measurement method that can measure the plasma density from the ion current and the electron temperature during the tone burst signal input.

**Index Terms**—Electron temperature, floating potential, ion current, Langmuir probe, plasma density.

## I. INTRODUCTION

LOW-PRESSURE plasma is widely used in semiconductor manufacturing processes, such as plasma chemical vapor deposition (CVD) [1]–[3], sputtering [4]–[6], and etching [7]–[9], and its research and development are still in progress at present [10]. In this process, it is necessary to control the physical properties of the plasma. In order to further develop the plasma of the above process, it is indispensable to construct a manufacturing system with the stable control of various plasma parameters (plasma density:  $n_0$ , electron temperature:  $T_e$ , ion flux:  $\Gamma_p$ , and so on). For example,  $n_0$  is an important parameter that indicates the condition of the ionized gas, and  $T_e$  is used as a measure of the energy of the plasma [11], [12]. Finally,  $\Gamma_p$  is an important parameter for controlling the ion flow in precision processing [13].

Various methods for measuring plasma parameters have been reported, including the electrostatic probe method [14], high-frequency probe method [15], [16], microwave measurement method [17], particle measurement method [18], spectroscopy method [19], and laser measurement method [20]. Among such research backgrounds, we have been studying the floating probe method [21], [22]. This method is different from

the Langmuir probe method [see Fig. 1(a)], which measures the current–voltage characteristics by directly inserting a probe inside the plasma and applying a dc voltage. As shown in Fig. 1(b), this method monitors the shift in the floating potential when an ac voltage is applied to the probe through an intermediary blocking capacitor. However, the limitation of the proposed method is its inability to measure more than one  $T_e$  when multiple  $T_e$ 's are involved.

In this study, we propose a new tone burst floating probe method that improves upon our previous floating probe method. The point different from the floating probe method is that instead of applying a continuous alternating current signal, a “tone burst signal” is applied, which applies an alternating current signal for a fixed period of one cycle and does not apply a remaining time. By inputting the tone burst signal, it is possible to measure  $T_e$  from the floating potential shift of the burst interval. Unlike the previous floating probe method, ion current ( $I_i$ ) can also be calculated from the time constant of the burst interval. Finally,  $n_0$  can also be calculated from the obtained  $T_e$  and  $I_i$ . We study these plasma parameters by using the tone burst floating probe method in various hollow cathode discharge processes.

## II. EXPERIMENTAL SETUP

The apparatus used in this research was the same as in our previous study [23]. Fig. 2 shows the apparatus for the proposed tone burst floating probe method. The electric circuit of a dc hollow cathode-type discharge tube is shown in Fig. 2(a). The discharge was performed using argon (99.9999%) at a total gas pressure of 0.3–0.9 torr and a current of 10–40 mA. The probe volt–ampere characteristics were measured using a digital electrometer (ADC 8252, ADC Corporation, Tokyo, Japan) with the switch set to ON, as shown in Fig. 2(a). The probe voltage was varied from  $-30$  to  $5$  V.

For the proposed tone burst floating probe method and simple previous floating probe method [21], [22], ac voltage was applied using a function generator (AFG 3022B, Tektronix Company, Tokyo, Japan) through an intermediary  $0.001\text{-}\mu\text{F}$  blocking capacitor. Sinusoidal tone burst waveforms with frequencies of  $50$  kHz and voltages from  $10$  to  $20$  V<sub>pp</sub> ( $5$ – $10$  V in amplitude) were applied and monitored using a digital oscilloscope (DPO 2024, Tektronix Company, Tokyo, Japan). Stable values were obtained at a frequency of  $50$  kHz in our previous study [21], [22]. The electrometer switch was turned off, as shown in Fig. 2(a),

Manuscript received October 28, 2020; revised May 5, 2021; accepted May 21, 2021. Date of publication June 9, 2021; date of current version July 22, 2021. The review of this article was arranged by Senior Editor S. Portillo. (Corresponding author: Shuichi Sato.)

The authors are with the Department of Electronic Engineering, Tokyo Denki University, Tokyo 120-8551, Japan (e-mail: s.sato@mail.dendai.ac.jp).

Color versions of one or more figures in this article are available at <https://doi.org/10.1109/TPS.2021.3084138>.

Digital Object Identifier 10.1109/TPS.2021.3084138

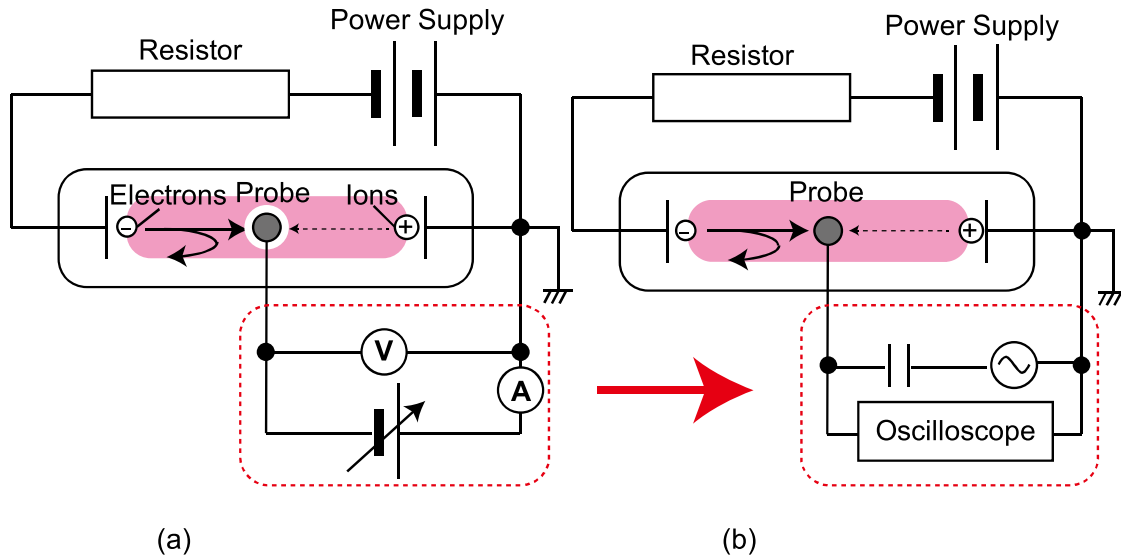


Fig. 1. Schematics of probe methods: (a) electric circuit of Langmuir probe method and (b) electric circuit of floating probe method.

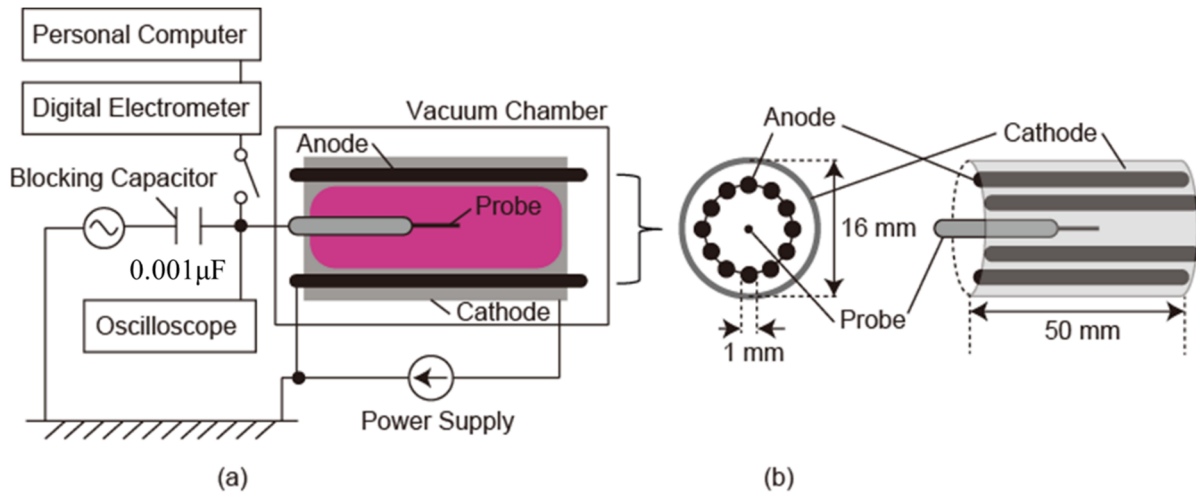


Fig. 2. Experimental setup for floating probe method: (a) electric circuit and (b) image of electrodes and probe.

because it was not necessary to measure the probe volt–ampere characteristics.

Schematic images of the probe, anode, and cathode are shown in Fig. 2(b). Twelve stainless steel rods, each having a 1.0-mm diameter, were used as anodes. A hollow cylinder with a 22-mm outer diameter, 16-mm inner diameter, and 50-mm length was used as a cathode. A thin tungsten wire with a diameter of 0.1 mm and a length of 2.0 mm was used as the probe. At the center of the hollow region, the probe made efficient contact with the discharge tube.

### III. RESULTS AND DISCUSSION

In Section III-A, experimental results obtained using the Langmuir probe, the previous floating probe, and tone burst floating probe methods are presented and analyzed.

#### A. Measurement of Electron Temperature Using Langmuir Probe Methods

Fig. 3 shows the discharge image and the probe's volt–ampere characteristics with a grounded plate. Fig. 3(a) shows

the probe's volt–ampere characteristic when the gas pressure was 0.3 torr and the current was 10 mA. This was the lowest pressure and current among these conditions. On the other hand, Fig. 3(b) shows that when the gas pressure was 0.9 torr and the current was 40 mA, this was the highest pressure and current among these conditions. The discharge current increased as the bias voltage increased and shows a nonlinear current–voltage curve. This nonlinear curve for the discharge current agreed with the measurements reported in an earlier study [21], [22]. The measured current–voltage characteristics were slightly slower for the low-voltage small current than for the high-voltage large current. The floating potentials ( $V_f$ ) at which the probe current became 0 had almost the same values:  $-2.87$  at 0.3 torr and 10 mA, and  $-2.89$  at 0.9 torr and 40 mA.

From the probe current–voltage characteristics,  $T_e$  was calculated using the Langmuir probe method and was assumed to follow the Maxwell distribution. As observed in (1),  $T_e$  depends on the derivative of the logarithm of the electron current ( $I_e$ ) with respect to the applied

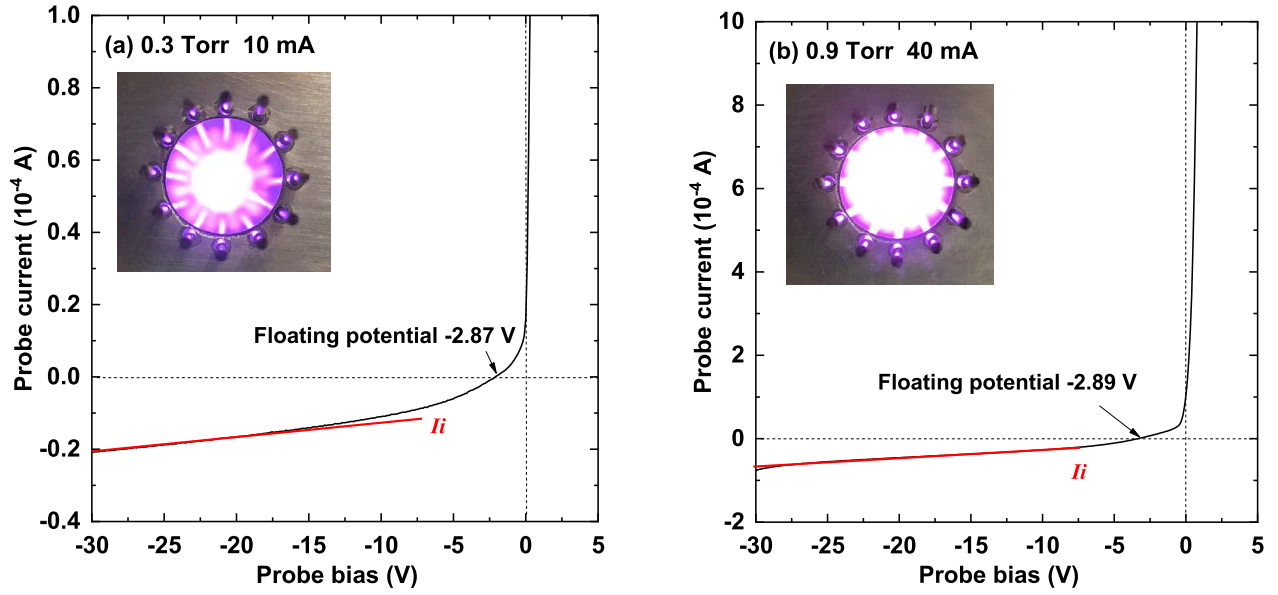


Fig. 3. Probe current as a function of probe bias voltage in hollow cathode-type discharge at (a) 10 mA and 0.3 torr and (b) 40 mA and 0.9 torr.

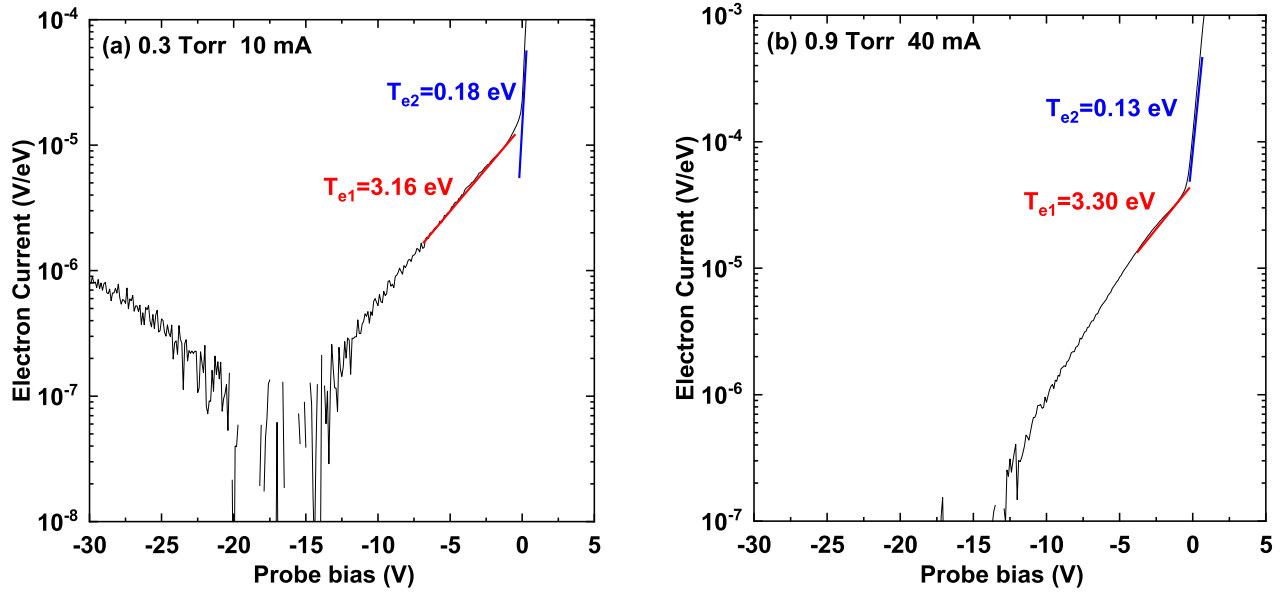


Fig. 4. Electron current as a function of probe bias voltage in hollow cathode-type discharge at (a) 10 mA and 0.3 torr and (b) 40 mA and 0.9 torr.

probe voltage  $V$

$$\frac{d}{dV} \ln I_e = \frac{e}{kT_e} \quad (1)$$

where  $I_i$  and  $I_e$  are combinations of the probe current ( $I_p$ ). It is necessary to subtract  $I_i$  from  $I_p$ . As a method of estimating  $I_e$  from  $I_p$ , the tangential line in the high-negative-bias voltage range as shown in Fig. 3(a) and (b) is considered as  $I_i$ ; then,  $I_e = I_p - I_i$ .

Fig. 4 shows the semilog plot of  $I_e$ . Two straight lines were observed from  $-6.9$  to  $-0.5$  V and from  $-0.2$  to  $0.3$  V, that is, two  $T_e$ 's were obtained. Comparing the results of 0.3 torr and 10 mA [Fig. 4(a)] and 0.9 torr and 40 mA [Fig. 4(b)], the high-tail electron temperature  $T_{e1}$  was 3.16 eV for 0.3 torr

and 10 mA, and 3.30 eV for 0.9 torr and 40 mA. On the other hand, the low bulk electron temperature  $T_{e2}$  was 0.18 eV for 0.3 torr and 10 mA, and 0.13 eV for 0.9 torr and 40 mA. The discharge pressure and current did not strongly depend on  $T_{e1}$  and  $T_{e2}$ .

Table I summarizes  $V_f$ ,  $T_{e1}$ , and  $T_{e2}$  among all discharge conditions. In this study, the same conditions were measured three times, and the mean value and standard error were calculated from there. Within our experimental range, discharges were performed under limited conditions. The conditions shown in Table I are the conditions that we were able to measure in this experiment. In addition, errors were introduced while calculating the slope of the tangential line to estimate  $I_i$ . This is because it is difficult to remove the influence of  $I_i$ .

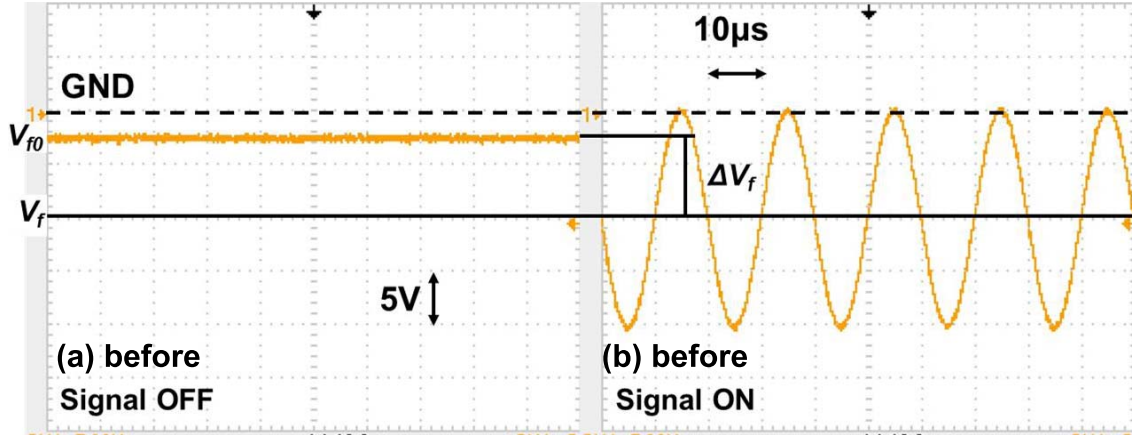


Fig. 5. Shift of floating potential by applied sinusoidal voltage (a) before and (b) after.

### B. Measurement of Electron Temperature Using Previous Floating Probe Methods

A summary of the previous floating potential ac diagnostic method is given as follows. This is a simple condensed version of the explanation from 2016 [21], [22].

Previously, we proposed a floating potential ac diagnostic method to measure  $T_e$ , as shown in Fig. 1(b). When a sinusoidal voltage ( $E\sin\omega t$ ) is applied to the probe voltage ( $V_p$ ) through the intermediary blocking capacitor, the current that permeates the sheath ( $I$ ) may be written as a function of  $I_i$  and  $I_e$  as

$$I(V_p + E\sin\omega t) = I_i - I_e(V_p + E\sin\omega t). \quad (2)$$

When the potential of plasma is  $V_s$ , (2) can be rewritten using Boltzmann's equation with  $T_e$  as

$$\begin{aligned} I(V_p + E\sin\omega t) &= I_i - I_{e0} \exp\left(\frac{e(V_p - V_s) + eE\sin\omega t}{kT_e}\right) \\ &= I_i - I_{e0} \exp\left(\frac{e(V_p - V_s)}{kT_e}\right) \\ &\quad \times \exp\left(\frac{eE}{kT_e} \sin\omega t\right) \end{aligned} \quad (3)$$

where  $I_{e0}$  is the saturated electron current. Equation (3) can be rewritten using a Fourier series expansion and harmonic analysis as follows:

$$\begin{aligned} I(V_p + E\sin\omega t) &= I_i - I_{e0} \exp\left(\frac{e(V_p - V_s)}{kT_e}\right) I_0\left(\frac{eE}{kT_e}\right) \\ &\quad - I_{e0} \exp\left(\frac{e(V_p - V_s)}{kT_e}\right) 2I_1\left(\frac{eE}{kT_e}\right) \sin\omega t \\ &\quad + I_{e0} \exp\left(\frac{e(V_p - V_s)}{kT_e}\right) 2I_2\left(\frac{eE}{kT_e}\right) \cos 2\omega t \\ &\quad + I_{e0} \exp\left(\frac{e(V_p - V_s)}{kT_e}\right) 2I_3\left(\frac{eE}{kT_e}\right) \sin 3\omega t \end{aligned} \quad (4)$$

where  $I_n(x)$  is a modified Bessel function of the  $n$ th order. When a sinusoidal voltage is applied to the probe through the intermediary blocking capacitor, (4) can be rewritten with a

zero dc component and  $V_p$  is equal to  $V_f$

$$I_i - I_{e0} \exp\left(\frac{e(V_f - V_s)}{kT_e}\right) I_0\left(\frac{eE}{kT_e}\right) = 0. \quad (5)$$

In addition,  $I_e$  is equal to  $I_i$  in the range of floating potential when the floating potential in the absence of a sinusoidal voltage is  $V_{f0}$

$$I_i - I_{e0} \exp\left(\frac{e(V_{f0} - V_s)}{kT_e}\right) = 0. \quad (6)$$

Based on (5) and (6), the difference between the floating potential as  $V_f - V_{f0}$ , which is the shift in the floating potential resulting from an applied sinusoidal voltage, can be represented as

$$\begin{aligned} I_{e0} \exp\left(\frac{e(V_{f0} - V_s)}{kT_e}\right) &= I_{e0} \exp\left(\frac{e(V_f - V_s)}{kT_e}\right) I_0\left(\frac{eE}{kT_e}\right) \\ \therefore \Delta V_f &= V_f - V_{f0} = -\frac{kT_e}{e} \ln\left\{I_0\left(\frac{eE}{kT_e}\right)\right\}. \end{aligned} \quad (7)$$

We call this method the ‘‘floating probe method’’ because it focuses on the floating potential and probe method.  $T_e$  can be calculated directly using this method without using volt-ampere characteristics. Therefore, this floating potential ac diagnostic method is effective. A method for measuring  $T_e$  by superimposing an RF signal was previously reported [24]. Our floating potential ac diagnostic method is different in which the dc component becomes 0 through the blocking capacitor based on (5). However, the proposed method is limited by its inability to measure more than one  $T_e$  when multiple  $T_e$ 's are involved.

As shown in Fig. 5,  $T_e$  can be calculated from the  $\Delta V_f$  shift in  $V_f$  by applying a sinusoidal wave signal to the previous floating probe method based on (7). A shift in the floating potential is a function of the amplitude of  $T_e$  and  $E$ . When  $V_f$  lacks an applied sinusoidal voltage,  $V_f$  can be replaced with  $V_{f0}$ .

Table I summarizes a shift in the floating potential and  $T_e$  calculated by (7) in the floating probe method under all discharge conditions. In the floating probe method, superimposing an RF signal includes a sinusoidal wave, rectangular



TABLE I  
 FLOATING POTENTIALS AND ELECTRON TEMPERATURES IN HOLLOW CATHODE DISCHARGE BY  
 LANGMUIR, FLOATING PROBE, AND TONE BURST FLOATING PROBE METHOD

Pressure (Torr)	Current (mA)	Langmuir Probe			Floating probe <sup>a)</sup>		Tone burst floating probe <sup>a)</sup>	
		$V_f$ (V)	$T_{e1}$ (eV)	$T_{e2}$ (eV)	$ \Delta V_f $ (V)	$T_e$ (eV)	$ \Delta V_f $ (V)	$T_e$ (eV)
0.3	10	-2.87±0.41	3.16±0.25	0.18±0.01	6.87±0.14	2.80±0.14	4.80±0.12	2.76±0.12
	20				N.D <sup>b)</sup>			
	30				N.D <sup>b)</sup>			
	40				N.D <sup>b)</sup>			
0.5	10	-2.15±0.22	3.51±0.18	0.58±0.23	7.72±0.39	2.07±0.31	5.53±0.35	2.04±0.32
	20	-2.51±0.47	3.52±0.10	0.71±0.31	7.16±0.22	2.54±0.20	4.73±0.07	2.59±0.22
	30				N.D <sup>b)</sup>			
	40				N.D <sup>b)</sup>			
0.7	10				N.D <sup>b)</sup>			
	20	-2.81±0.43	3.19±0.14	0.49±0.30	7.32±0.22	2.39±0.19	4.86±0.27	2.39±0.21
	30	-3.43±0.05	3.20±0.13	0.35±0.16	6.38±0.20	3.31±0.21	3.53±0.24	3.32±0.20
	40				N.D <sup>b)</sup>			
0.9	10				N.D <sup>b)</sup>			
	20	-2.36±0.24	3.34±0.12	0.22±0.01	7.18±0.29	2.53±0.26	5.00±0.20	2.44±0.32
	30	-2.51±0.25	3.45±0.08	0.20±0.02	6.94±0.31	2.75±0.28	4.27±0.07	2.88±0.21
	40	-2.79±0.34	3.30±0.03	0.20±0.03	6.36±0.02	3.30±0.05	3.73±0.07	3.38±0.05

a) Frequency: 50 kHz at 20 V<sub>pp</sub>

b) Not Determined

wave, and triangular waves. In this study, we used a 20-V<sub>pp</sub> and 50-kHz sinusoidal wave whose  $T_e$  was a converged value based on previous reports [21], [22].  $|\Delta V_f|$  and the effective  $T_e$  were 6.87 V and 2.80 eV at 0.3 torr and 10 mA, and 6.36 V and 3.30 eV at 0.9 torr and 40 mA, respectively. Compared with  $T_e$  in the Langmuir probe method, only one  $T_e$  can be calculated using the floating probe method. The value is close to the high-tail  $T_{e1}$  value. Because high-tail  $T_{e1}$  has a larger amount of plasma energy than  $T_{e2}$ ,  $T_{e1}$  is an industrially important plasma parameter.

### C. Measurement of Electron Temperature Using Tone Burst Floating Probe Method

In the floating probe method, the value of  $V_{f0}$  (signal OFF) shown in Fig. 5 gradually shifts because the discharge is unstable. The measurement conditions change from time to time. Therefore, it is necessary to switch the signal ON and OFF instantly because the measurement time is so short. To switch instantaneously, we used a new tone burst waveform. This method is called the “tone burst” floating probe method. As shown in Fig. 6, signal ON and signal OFF are repeated by applying a sine-wave tone burst signal. The median floating potential when the signal is ON is  $V_f'$ . When the signal turns off, positive ions flow into the negatively charged blocking capacitor, and the probe potential moves in the direction of the positive voltage and becomes a constant potential  $V_{f0}'$ .

$$\Delta V_f = |V_f' - V_{f0}'| = \frac{kT_e}{e} \ln \left\{ I_0 \left( \frac{eE}{kT_e} \right) \right\}. \quad (8)$$

$T_e$  can be calculated from the same equation [see (7)]. The shift in floating potential between the signal ON and OFF can be measured average value of signal ON within one cycle and steady voltage of signal OFF, as shown in Fig. 6. Therefore, even when the plasma is temporally unstable,  $T_e$  can be precisely calculated.

Fig. 7 shows the input voltage dependence of  $T_e$  calculated by the tone burst floating probe method when the gas pressure was 0.9 torr and the current was 40 mA. In a range lower than 10 V<sub>pp</sub>,  $T_e$  could not be observed because a precise  $\Delta V_f$  was not obtained, that is, when burst waves were applied, there was no shift in the floating potential. Therefore,  $T_e$  could be observed in the range of 10–20 V<sub>pp</sub>. As the frequency increased at the input waveforms,  $T_e$  decreased and converged to 3 eV. The value was close to the high-tail  $T_{e1}$  value, as with the previous floating probe method. This electron temperature also showed good agreement with the electron temperature of the floating probe method. A more accurate electron temperature was required because the switching time required by the floating probe method was eliminated.

Fig. 8 shows a graph comparing  $T_e$  of the tone burst floating probe method ( $T_{TBF}$ ) shown in Table I and  $T_e$  of the floating probe method ( $T_{FP}$ ). It can be seen from Fig. 8 that the tone burst floating probe method is consistent with the measurement results of the floating probe method.

Table I summarizes the shift in the floating potential and the effective  $T_e$  calculated by (8) in the tone burst floating probe method under all discharge conditions. Interestingly, as the pressure and current increased,  $T_e$  in the tone burst floating

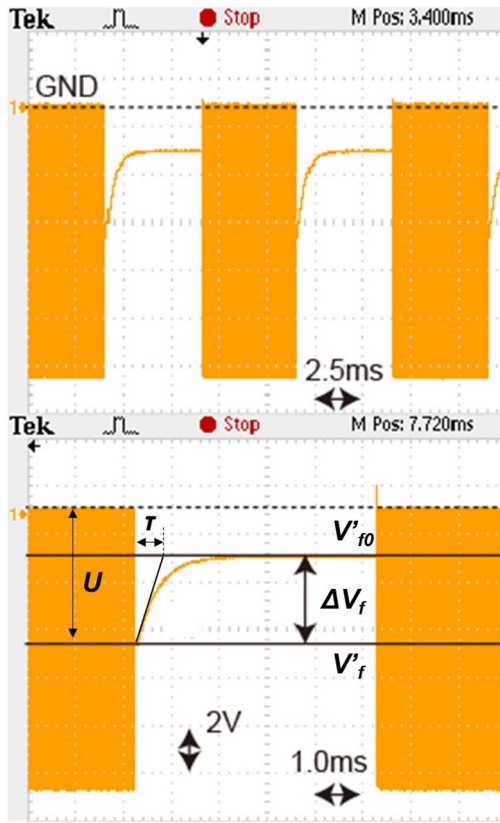


Fig. 6. Shift of floating potential by applied tone burst sinusoidal voltage.

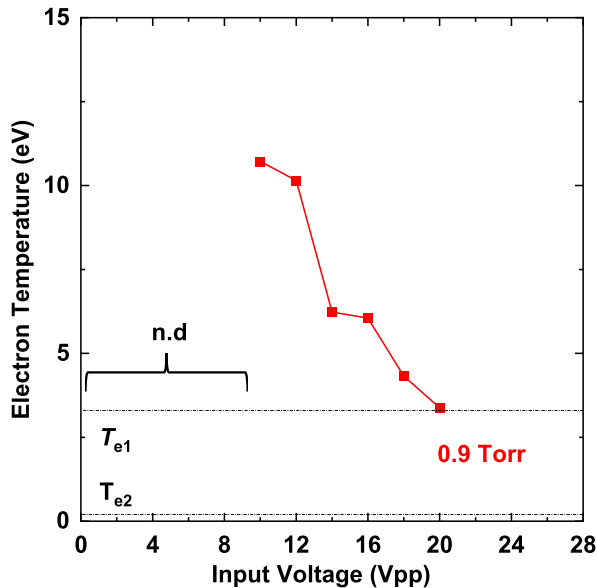


Fig. 7. Electron temperatures in response to tone burst sinusoidal waves as a function of input voltage at 50 kHz.

probe method agreed with that in the Langmuir probe method. The value converged to 3.0–4.0 eV. On the other hand, when the discharge pressure and current were low, the value in the tone burst and previous floating probe methods was lower than that in the Langmuir probe method. This is because the plasma condition changed drastically when the discharge pressure and

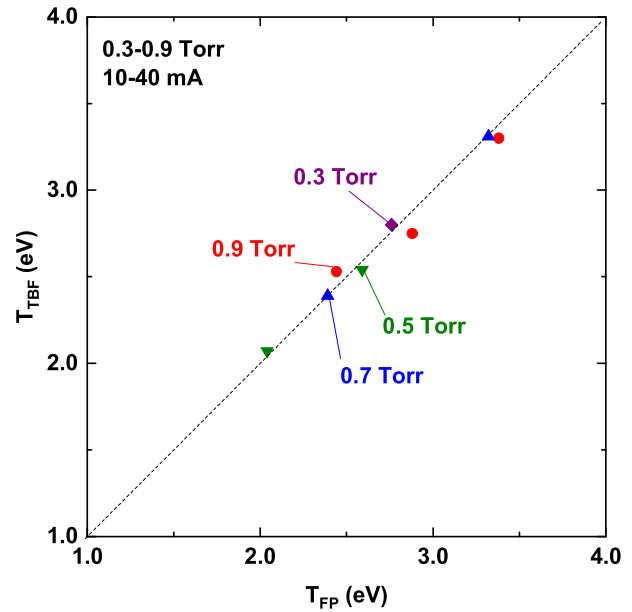


Fig. 8. Electron temperature of the tone burst floating probe method and electron temperature of the floating probe method.

current were low. Since the probe is not sufficiently exposed to the plasma in this condition,  $T_e$  in the tone burst floating probe method changed from time to time, that is, this method measures  $T_e$  in an unstable state of plasma.

#### D. Measurement of Various Plasma Parameters by Tone Burst Floating Probe Method

Various plasma parameters except for the effective  $T_e$  were also calculated by the novel tone burst floating probe method. This is the difference between the previous floating probe method and the new tone burst floating probe method. In this section, other parameters (time constant  $\tau$ ,  $I_i$ , and  $n_0$ ) measured or calculated by the tone burst floating probe method are presented.

As shown in Fig. 6, the time constant  $\tau$  indicates the initial slope from the signal ON to the signal OFF.  $\tau$  was observed because the ion current to the probe discharges the charge from the blocking capacitor. The first  $I_p$  can be measured in the probe and  $I_e$  can be neglected at large negative probe potential, so  $I_p$  can be represented as the capacitance of blocking capacitor  $C$  dependent on  $\Delta V_f$ . When a sufficiently large alternating voltage is applied to the probe, the probe is biased to a large negative voltage, and at the moment of signal OFF, it can be considered that only charged particles flow into the probe are ions. If this is the ion current  $I_i$ , it is equal to the current flowing in the blocking capacitor, that is, assuming that the moment of signal OFF is  $t = 0$

$$I_i = I_p(t) |_{t=0} = C \frac{dV_f}{dt} \Big|_{t=0} \approx C \frac{\Delta V_f}{\tau}. \quad (9)$$

As the floating voltage rises, the electron current also flows in, so the rate of change of the floating voltage decreases and converges to the steady-state value. This steady-state value should be the floating voltage  $V_{f0}$  when there is no signal.

TABLE II

TIME CONSTANT, ION CURRENT, AND PLASMA DENSITY IN HOLLOW CATHODE DISCHARGE BY THE TONE BURST FLOATING PROBE METHOD

Pressure (Torr)	Current (mA)	Time constant $\tau$ (ms)	Ion current $I_i$ ( $\times 10^{-6}$ A)	Plasma density $n_0$ ( $\times 10^{10}$ cm $^{-3}$ )
0.3	10	0.88 $\pm$ 0.11	4.45 $\pm$ 0.56	1.78 $\pm$ 0.26
0.5	10	0.65 $\pm$ 0.04	5.10 $\pm$ 0.89	3.30 $\pm$ 0.72
	20	0.35 $\pm$ 0.06	11.7 $\pm$ 2.43	4.90 $\pm$ 1.23
0.7	20	0.35 $\pm$ 0.03	11.3 $\pm$ 0.69	4.84 $\pm$ 0.26
	30	0.21 $\pm$ 0.04	14.2 $\pm$ 2.62	5.18 $\pm$ 1.01
0.9	20	0.44 $\pm$ 0.05	9.23 $\pm$ 1.06	3.96 $\pm$ 0.52
	30	0.25 $\pm$ 0.02	13.8 $\pm$ 1.10	5.39 $\pm$ 0.58
	40	0.29 $\pm$ 0.03	10.6 $\pm$ 1.30	3.81 $\pm$ 0.46

Therefore, the time of signal OFF needs to be sufficiently longer than  $\tau$  in this tone burst floating probe method. In addition, it is necessary to select a blocking capacitor with a low capacitance so that the floating potential changes in a short time.

Finally,  $n_0$  can also be calculated by using this tone burst floating probe method. The ion current to the probe immediately after signal OFF is the Bohm velocity,  $I_i$  can be calculated by (10) using the positive ion mass  $M$  and probe area  $S$  [23]

$$I_i = e \cdot 0.61n_0 \sqrt{\frac{kT_e}{M}} \cdot S \approx \frac{C \Delta V_f}{\tau}. \quad (10)$$

Equation (10) can be transformed into (11) and

$$n_0 \approx \frac{1}{0.61S} \sqrt{\frac{M}{kT_e}} \cdot \frac{C \Delta V_f}{e\tau} \quad (11)$$

where  $n_0$  can be calculated from  $T_e$  and  $\tau$ .

Table II summarizes  $\tau$ ,  $I_i$ , and  $n_0$  in the tone burst floating probe method under all discharge conditions. When the floating potential shifted to a constant,  $\tau$  varied from 0.21 to 0.88 ms, and the value tripled. The higher the effective  $T_e$ , the lower  $\tau$  when the discharge pressure and current were high.  $I_i$  can be calculated from (10) and the obtained  $T_e$  and  $n_0$  when  $C$  is 0.001  $\mu$ F and  $e$  is  $1.602 \times 10^{-19}$  C.  $I_i$  ranged from 4.45 to  $14.2 \times 10^{-6}$  A. By contrast, with regard to  $\tau$ , as the discharge current increased,  $I_i$  increased. This tendency was in good agreement with that in the literature [13]. Finally,  $n_0$  was calculated from (11) when  $S$  was  $1.26 \times 10^{-5}$  m $^2$  and  $M$  was  $6.68 \times 10^{-26}$  kg.  $n_0$  ranged from 1.78 to  $5.39 \times 10^{10}$  cm $^{-3}$ . The value of  $n_0$  was also low when the discharge pressure, current, and  $I_i$  were low; otherwise, the values were almost the same. Unlike  $I_i$ ,  $T_e$  did not strongly depend on  $n_0$ .

Thus, the proposal tone burst floating probe method has an advantage whereby the shift in the floating potential can be found by means of only "one cycle" of the tone burst wave. This, therefore, considers most of the advantages of our previous floating probe method.

In addition, this method has the following other advantage.

1) It solves the effect of the time change of  $V_f$  or  $V_S$ .

- 2) The approximate spatial potential can be determined as the positive peak signal voltage.
- 3)  $I_i$  can be determined from the time change of  $V_f$ .
- 4)  $n_0$  can be determined from the effective  $T_e$  and  $I_i$ .

#### IV. CONCLUSION

$T_e$ ,  $I_i$ , and  $n_0$  were calculated using a tone burst floating probe method through a hollow cathode-type discharge tube. This was an improvement on our previous floating probe method.  $T_e$  was rapidly calculated from a shift in the floating potential of the burst interval when a tone burst signal was applied to a probe through an intermediary blocking capacitor. Then,  $I_i$  and  $n_0$  were calculated from  $\tau$  to shift the floating potential between signals ON and OFF. Since  $T_e$  was changed from time to time when the discharge pressure and current were low,  $T_e$  in the tone burst floating probe method was not in agreement with that in the Langmuir probe method. However,  $T_e$  in the tone burst floating probe method agreed with that in the Langmuir probe method when the discharge pressure and current were high, that is, this tone burst floating probe method can measure  $T_e$  in an unstable state of plasma.

#### REFERENCES

- [1] M. Chhowalla *et al.*, "Growth process conditions of vertically aligned carbon nanotubes using plasma enhanced chemical vapor deposition," *J. Appl. Phys.*, vol. 90, no. 10, pp. 5308–5317, Nov. 2001.
- [2] K. L. Choy, "Chemical vapour deposition of coatings," *Prog. Mater. Sci.*, vol. 48, no. 2, pp. 170–157, 2003.
- [3] P. G. Pai, S. S. Chao, Y. Takagi, and G. Lucovsky, "Infrared spectroscopic study of siox films produced by plasma enhanced chemical vapor-deposition," *J. Vac. Sci. Technol. A, Vac. Surf. Films*, vol. 4, no. 3, pp. 689–694, Jun. 1986.
- [4] P. K. Chu, J. Y. Chen, L. P. Wang, and N. Huang, "Plasma-surface modification of biomaterials," *Mater. Sci. Eng. R, Rep.*, vol. 36, nos. 5–6, pp. 143–206, Mar. 2002.
- [5] J. Hopwood, "Review of inductively coupled plasmas for plasma processing," *Plasma Sources Sci. Technol.*, vol. 1, no. 2, pp. 109–116, May 1992.
- [6] P. H. Mayrhofer, C. Mitterer, L. Hultman, and H. Clemens, "Microstructural design of hard coatings," *Prog. Mater. Sci.*, vol. 51, no. 8, pp. 1032–1114, Nov. 2006.
- [7] J. W. Coburn and H. F. Winters, "Ion-assisted and electron-assisted gas-surface chemistry important effect in plasma-etching," *J. Appl. Phys.*, vol. 50, no. 5, pp. 3189–3196, 1979.

- [8] S. J. Pearton, D. P. Norton, K. Ip, Y. W. Heo, and T. Steiner, "Recent progress in processing and properties of ZnO," *Prog. Mater. Sci.*, vol. 50, no. 3, pp. 293–340, Mar. 2005.
- [9] S. J. Pearton, J. C. Zolper, R. J. Shul, and F. Ren, "GaN: Processing, defects, and devices," *J. Appl. Phys.*, vol. 86, no. 1, pp. 1–78, Jul. 1999.
- [10] I. Adamovich *et al.*, "The 2017 plasma Roadmap: Low temperature plasma science and technology," *J. Phys. D: Appl. Phys.*, vol. 50, no. 32, 2017, Art. no. 323001.
- [11] P. Franz *et al.*, "Experimental investigation of electron temperature dynamics of helical states in the RFX-Mod reversed field pinch," *Nucl. Fusion*, vol. 53, no. 5, Apr. 2013, Art. no. 053011.
- [12] E. Passoth, P. Kudrna, C. Csambal, J. F. Behnke, M. Tichý, and V. Helbig, "An experimental study of plasma density determination by a cylindrical Langmuir probe at different pressures and magnetic fields in a cylindrical magnetron discharge in heavy rare gases," *J. Phys. D: Appl. Phys.*, vol. 30, no. 12, pp. 1763–1777, Jun. 1997.
- [13] N. S. J. Braithwaite, J. P. Booth, and G. Cunge, "A novel electrostatic probe method for ion flux measurements," *Plasma Sources Sci. Technol.*, vol. 5, no. 4, pp. 677–684, Nov. 1996.
- [14] H. M. Mott-Smith and I. Langmuir, "The theory of collectors in gaseous discharges," *Phys. Rev.*, vol. 28, pp. 727–763, Oct. 1926.
- [15] H. Kokura, K. Nakamura, I. P. Ghanashev, and H. Sugai, "Plasma Absorption Probe for Measuring Electron Density in an Environment Soiled with Processing Plasmas," *Jpn. J. Appl. Phys.*, vol. 38, no. 9R, p. 5262, 1999.
- [16] K. Takayama, H. Ikegami, and S. Miyazaki, "Plasma resonance in a radio-frequency probe," *Phys. Rev. Lett.*, vol. 5, no. 6, pp. 238–240, 1960.
- [17] M. K. Thumm and W. Kasperek, "Passive high-power microwave components," *IEEE Trans. Plasma Sci.*, vol. 30, no. 3, pp. 755–786, Jun. 2002.
- [18] J. C. Hosea, F. C. Jobses, R. L. Hickok, and A. N. Dellis, "Rotation and structure of low-frequency oscillations inside the ST-tokamak plasma," *Phys. Rev. Lett.*, vol. 30, no. 18, pp. 839–842, Apr. 1973.
- [19] J. Booth and G. Hancock, "Radical kinetics in processing plasmas: Optical diagnostics of gas phase and surface reactions," in *Materials Science Forum*, vol. 140. Switzerland: Trans Tech Publications, 1993, pp. 219–234. [Online]. Available: <https://www.resurchify.com/impact/details/28700>
- [20] H. C. Liu, X. L. Mao, J. H. Yoo, and R. E. Russo, "Early phase laser induced plasma diagnostics and mass removal during single-pulse laser ablation of silicon," *Spectrochim. Acta B, Atomic Spectrosc.*, vol. 54, no. 11, pp. 1607–1624, Nov. 1999.
- [21] S. Nodomi, S. Sato, and M. Ohuchi, "Electron temperature measurement by floating probe method using AC voltage," *Plasma Sci. Technol.*, vol. 18, no. 11, p. 1089, 2016.
- [22] S. Sato, H. Kawana, T. Fujimine, and M. Ohuchi, "Frequency dependence of electron temperature in hollow cathode-type discharge as measured by several different floating probe methods," *Plasma Sci. Technol.*, vol. 20, pp. Art. no. 085405, 2018.
- [23] M. A. Lieberman, and A. J. Lichtenberg, *Principles of Plasma Discharges and Materials Processing*. New York, NY, USA: Wiley, 2005.
- [24] M. H. Lee, S.-H. Jang, and C. W. Chung, "Floating probe for electron temperature and ion density measurement applicable to processing plasmas," *J. Appl. Phys.*, vol. 101, no. 3, 2007, Art. no. 033305.